In situ Brillouin scattering study of water in high pressure and high temperature conditions

2007 J. Phys.: Condens. Matter 19 425205

(http://iopscience.iop.org/0953-8984/19/42/425205)

IOP PUBLISHING JOURNAL OF PHYSICS: CONDENSED MATTER

J. Phys.: Condens. Matter **19** (2007) 425205 (9pp) doi:10.1088/0953-8984/19/42/425205

In situ Brillouin scattering study of water in high pressure and high temperature conditions

Fangfei Li, Qiliang Cui, Tian Cui, Zhi He, Qiang Zhou and Guangtian Zou

National Lab of Superhard Materials, Jilin University, 130012, People's Republic of China

E-mail: zhouqiang@mail.jlu.edu.cn

Received 3 August 2007
Published 18 September 2007
Online at stacks.iop.org/JPhysCM/19/425205

Abstract

Experimental studies of liquid water are of particular interest because of the unusual behavior of most of its physical properties. The *in situ* high pressure and high temperature Brillouin scattering technique has been used to examine the sound velocity and elastic properties of water; we present experimental data for the velocities of liquid water under these conditions. The velocity dispersion with pressure and temperature is presented; besides the discontinuous behavior in density dependence of the elastic constant below 353 K revealed before, which was located at the domain where the low density water transforms to the high density water, the pressure evolution of velocity at higher temperatures above 453 K also exhibits different change behaviors during compression; a velocity descent with increasing temperature at pressures below about 2.0 GPa was observed, but no obvious drop was seen in the higher pressure region. The elastic constants were calculated based on the velocities and a similar trend of changes with pressure was found. The temperature dependences of velocities measured along the quasi-isobaric lines give a consistent result. With analysis of the local structure of liquid water, it is suggested that these observations denote a reflection of the density changes which are induced by hydrogen bonding configuration modifications under high pressure and high temperature conditions. We discuss details of the experimental observations and analyze the mysterious physical properties of liquid water, combining other experiments and theory calculations.

(Some figures in this article are in colour only in the electronic version)

1. Introduction

Water is the most abundant substance on our planet and has been intensively studied over centuries, but most of its anomalous physical properties are still not well understood [1].

Although hydrogen bonds are much weaker than conventional chemical bonds, they are really the reason why water possesses versatile phases of crystalline and two or more amorphous states [2–5]. Recently the main interest has been focused on the controversy of a possible liquid–liquid first-order phase transition and on the experimental observation of a second critical point in supercooled water [6–8]. Due to the homogeneous crystallization, the ergodic to nonergodic transition from the supercooled liquid to the glass cannot be studied continuously as a function of temperature. On the other hand, molecular dynamics (MD) studies suggest the structures of the liquid and amorphous states are continuous [9], and the site–site radial distribution functions for low density amorphous ice (LDA) and high density amorphous ice (HDA) using neutron diffraction and hydrogen isotope substitution have suggested that the structure of liquid water is indeed quite analogous to HDA [10]. To explain the observed behavior under pressure, there is wide consensus that the low density water (LDW) and high density water (HDW) may be the high temperature manifestations of LDW and HDW, respectively [8]. However, the discovery of the third amorphous ice, very high density amorphous (VHDA) [11], indicated that, although indirectly, there may be a possibility of more than one liquid–liquid phase transition between amorphous water phases. The possibility of several liquid–liquid phase transitions in one-component isotropic fluid can be assumed, as not a single but several crystalline phases may melt directly to a liquid, and different local orders in the liquid phases may originate from the structure of the corresponding crystalline phases. The multiplicity of the liquid–liquid phase transitions in supercooled water obtained in computer simulations has received strong support from the recent experimental observation of two phase transitions between amorphous ices [12, 13], and four amorphous water phases (I–IV) obtained in simulations have been assigned to three kinds of amorphous ices [5].

The multiple liquid–liquid phase transitions in a one-component isotropic fluid were obtained in the simulations of the phase diagrams of several water models [5, 12, 14], but still not observed in supercooled water in experiments. Although the liquid–liquid phase transitions in supercooled water have been extensively studied by various experimental and simulation methods, investigations of the liquid–liquid transformation in the stable liquid region have been comparably rare. The transition from low density to high density water has been predicted by classical molecular dynamics calculations and observed from Brillouin spectroscopic study [15, 16], but the predictions on the thermodynamic boundary between LDW and HDW forms was conflicting with that given by Raman spectroscopic study [17]. In the high temperature regions the local structure in liquid water has been measured by x-ray absorption spectroscopy (XAS) and x-ray Raman scattering (XRS), which indicated that upon heating from 25 to 90 °C some of the molecules change from tetrahedral environments to two hydrogen-bonded configurations [18]. The neutron diffraction study demonstrated that with increasing density the hydrogen bonds remain intact but distort only a little the tetrahedral first-neighbor coordination, and stated that liquid water at high densities should be structurally related to VHDA rather than ice VII [19]. In this paper, we present a velocity and elastic investigation of water in the stable liquid region under high temperature and high pressure conditions. The velocity variation along the isothermal lines and the quasi-isobaric lines are outlined and analyzed in detail.

2. Experimental details

The high temperature and high pressure (HTHP) conditions are generated by a modified Merrill–Bassett type four-screw diamond anvil cell (DAC) with a small resistance heater pasted on the side face of the diamond [16]. To prevent the reaction of the gasket in water under extreme conditions, rhenium was selected as gasket material. The rhenium gasket was pre-

indented and a hole drilled in the center of the pre-indented area; distilled and deionized water was loaded into the hole together with a small chip of ruby for the pressure scale [20]. The temperature was measured by a chromel–alumel thermocouple attached to the side face of the diamond.

The Brillouin spectra were collected by a newly developed (3 + 3)-pass tandem Fabry–Perot interferometer, which was designed by J R Sandercock. A narrow frequency (<5 MHz) green (532 nm) laser was used as the Brillouin excitation source. The laser is a solid-state diode-pumped, frequency-doubled Nd:vanadate laser, which is made by Coherent Company. The sample seat can fit the diamond cell in back-scattering geometry and allow *in situ* continuous compression under HTHP conditions. The sound velocity V can be obtained from the Brillouin shift $\Delta\omega_{\mathrm{B}}$ (in GHz) using the following expression [21]:

$$\Delta\omega_{\mathrm{B}} = \frac{2nV}{\lambda_0}\sin\theta, \tag{1}$$

in this expression, λ_0 is the wavelength of the exciting radiation, n is the refractive index, and 2θ is the scattering angle between incident light and scattered light. For the back-scattering geometry it is expressed as

$$\Delta\omega_{\mathrm{B180}} = \frac{2nV_{180}}{\lambda_0}, \tag{2}$$

where 180 indicates the angle between the incident and scattered beams.

The velocities of liquid water were measured along two different experimental paths; one is the isothermal line and the other is along quasi-isobaric line. We heated the sample up to a constant temperature, and then increased the pressure step by step and measured the pressure evolution of velocity until it solidified finally. The solidifying process can be monitored either by microscope or by analyzing the data of the Brillouin scattering measurement. Taking into account the existence of a temperature gradient around the sample chamber, the temperature dispersion between the anvil center and the side face of the diamond could not be ignored. The temperatures and pressures of the solidification points of water were then compared with the melting line of water for calibration [22, 23]. By this method, the actual pressure and temperature of the sample could be exactly determined. Another path is along the quasi-isobaric line, where we leave the diamond anvil cell at a scheduled pressure and then increase the temperature gradually. The real pressure and temperature were also corrected by the melting line of water at the two phase coexistence points, and a corresponding temperature correction line was obtained. In the experiments the temperature was controlled by a feedback power with the uncertainty of 1 K. Pressure was estimated on the ruby scale with a precision better than 0.05 GPa [20]. The temperature and pressure dependences of the ruby fluorescence were assumed to be independent of each other [24].

3. Results and discussion

For the Brillouin scattering measurements in a liquid only one longitudinal mode can be observed and it is sensitive to the phase transition between solid and liquid; this is useful to correct the temperature in the sample chamber. Typical Brillouin scattering spectra are presented in figure 1. As shown, the melting procedure can be clearly observed as the longitudinal mode belonging to the liquid phase grows gradually with increasing temperature, while that belongs to solid phase decreases and finally disappears after melting. Pressure evolutions of the Brillouin frequency shifts in liquid water along several isotherms have been measured; as the measurements were performed in the back-scattering geometry, we should have the knowledge of the refractive index to calculate the corresponding velocities. An

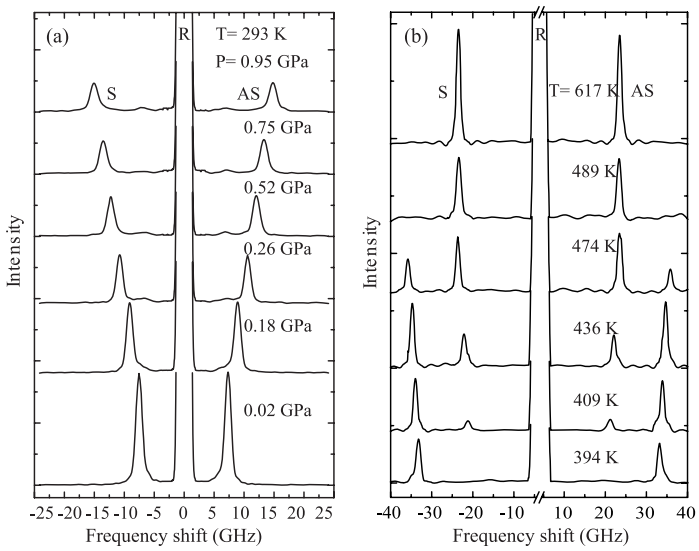

Figure 1. Representative Brillouin scattering spectra of water under high pressures and high temperatures. (a) The Brillouin frequency shift changes with pressure at 293 K. (b) The Brillouin frequency shift changes with temperature; the melting procedure can be clearly observed as the branch belonging to the liquid mode grows gradually with increasing temperature.

approximation method was used to get the pressure dependence of velocities as done in an earlier paper [16]. In this process we made an approximation to the refractive index by fitting the quantity $(n^2 - 1)/(n^2 + 2)$ calculated from all experimental data to a linear dependence on density, and then a full line extrapolation was used to give us the refractive index as a function of density. Combined with the pressure evolution of density at a given temperature, which was calculated from the equation of state given by Saul and Wagner, the relations between refractive index and pressure can be obtained [25–27].

Pressure evolutions of velocities along several isotherms are presented in figure 2. The temperature ranged from 433 to 564 K and the velocity changes can be observed; below 453 K the isotherms have been presented in the inset of figure 2 and discussed in detail in another work [16]. At low temperatures the velocities measured before increase monotonically with pressure but hardly move with temperature changes, while with the temperature increases to higher regions we can see it begin to descend slowly in the low pressure regime lower than about 2.0 GPa, but meanwhile no obvious drop of the velocity was observed in the high pressure regime. The elastic constant calculated from these velocities show a similar change behavior. As the transformation from LDW to HDW occurs, an increase in the oxygen coordination and variation in angular distributions was predicated; the behavior we observed here may reflect another possible modification of the local hydrogen configurations with a subtle change in density.

In order to get a direct observation of the temperature dependence of velocities in liquid water, we measured velocity evolutions along the quasi-isobaric lines. After the sample was sealed in the diamond anvil cell, it was pressed to a scheduled pressure and then the temperature was increased slowly. Due to the subtle pressure changes in the sample chamber when heating, a three-dimensional illustration of the velocity at different pressure and temperatures is presented in figure 3. As mentioned above, in the process of temperature correction we

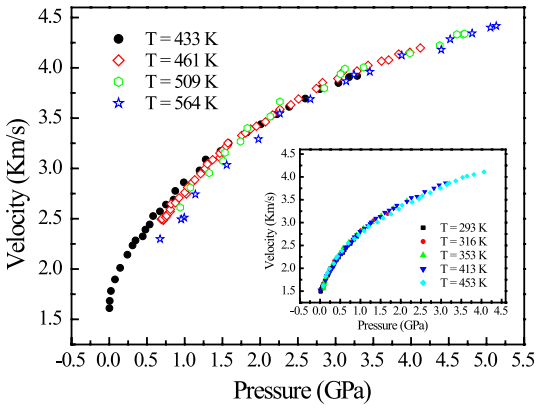

Figure 2. Pressure evolutions of velocities along different isotherms from 433 to 564 K. With the increasing temperature a gradual decrease of the velocity in the low pressure regime can be observed, while no obvious drop of the velocity was observed in the high pressure regime. In the inset, we present the comparisons of velocities along other isotherms at low temperatures in an early study; they increase monotonically with pressure but hardly move with the temperature changes, comparatively.

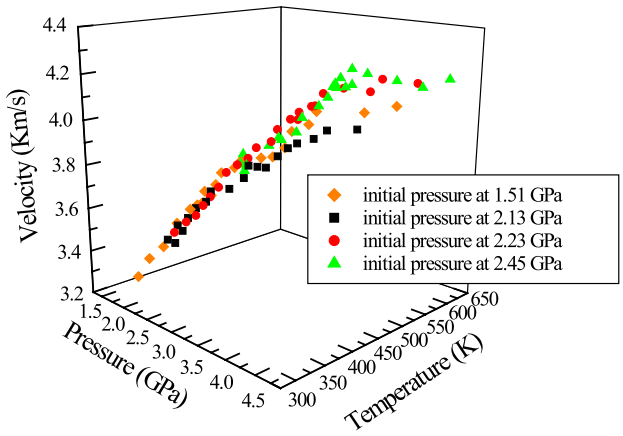

Figure 3. Three-dimensional illustrations of the velocity changes at different pressures and temperatures. For the ice VI melting procedure the temperature is corrected based on the linear relationship obtained from the melting curve of ice VII.

compare the solid–liquid coexistence points with the melting curve of ice VII, then a linear relationship between the temperatures at the thermal couple position and in the sample chamber can be obtained, and this relationship was applied immediately to calculate the true temperature for the ice VI melting procedure. The correction relationship was illustrated in the inset of figure 4(a). When the temperature increases in a uniform phase, either pure solid or liquid phase, the pressure changes in the sample chamber are extremely slight. During the melting process the pressure is elevated little by little as the temperature rises continuously; as the melting procedure begins, a part of the ice converts to the liquid state and its volume expands, and this causes the pressure to increase gradually during melting process. This procedure can be clearly observed in figure 4(a), the pressure–temperature (P–T) projection of the three-dimensional illustration.

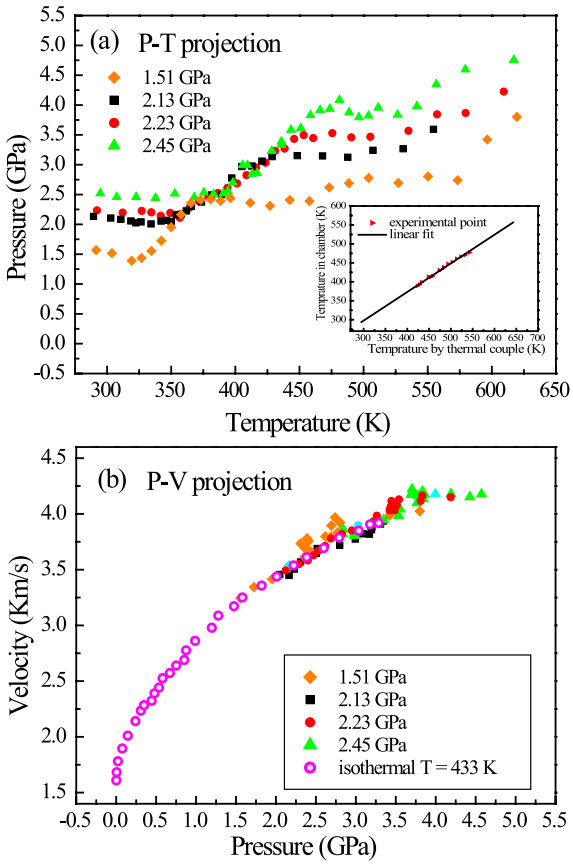

Figure 4. Pressure–temperature projection (a) and pressure–velocity projection (b) of the three-dimensional illustration in figure 3. Four experiment groups are indicated by different symbols (solid symbols) and a velocity evolution along an isotherm at 433 K (open circles) is shown as a guide line for the eyes and to provide a reference for comparing the temperature dependence of velocity in the same pressure region. In the inset of (a) a linear relationship between the temperatures at the thermal couple position and in the sample chamber is illustrated.

In figure 4(b) the pressure–velocity (P–V) projection of the three-dimensional illustration is presented. A velocity evolution along the isotherm at 433 K (open circles) is shown as a guide line for the eyes and provides a reference for comparing the temperature dependence of velocity in the vicinal pressure region. As shown in figure 4, the same experimental points are presented by the same symbols in both (a) and (b) together with figure 3. In each group we can see that in the process of melting the velocity variations match up to that along the isothermal line at 433 K; when the melting is completed its velocity rises slightly compared to the isotherm. The obvious increase of Brillouin frequency shift signals of both liquid and solid during melting can also be seen in figure 1, but only a slight change occurs at high temperatures, comparatively. If we come back to the results obtained from isothermal path measurements, it is clear that these two results are consistent with each other; in the high pressure regime just above about 2.0 GPa no drop of velocity was observed with temperature increase, but a little rise as the temperature grows higher and higher.

In order to gain a deeper insight into the mechanism of velocity changes in liquid water under HPHT conditions we should take into account its hydrogen bonding configuration

changes. The hydrogen bonding in water favors a tetrahedral arrangement of nearest water molecules, which results in a three-dimensional random hydrogen-bonded network characterized by a relatively open structure. Upon pressing, a collapse of the second neighbor shell towards the first neighbor shell and a breaking of the hydrogen bond between these two shells have been suggested to interpret the transformation form LDW to HDW by neutron diffraction studies [10, 28, 29]. On the other hand, classical molecular dynamics calculations suggest the important role of nonbonded molecules regarded as interstitial molecules in the two-form transformation, it means that at high pressure other second-shell molecules are closer to the central one than the second-shell molecules at ambient pressure [15]. Although different conclusions are drawn from these studies, they reveal the possible existence of HDW, which at a pressure of a few kilobars gradually evolves at the expense of LDW. In the spectral studies, Raman and Brillouin spectra have given conflicting predictions on the thermodynamic boundary between LDW and HDW forms [16, 17]. Consistent individuation of LDW and HDW basins obtained from molecular dynamics calculations and Brillouin studies allows us to consider that the velocity and elastic measurements are sensitive to detect density changes due to the local structural modifications in liquid water. In this study, the different behaviors in pressure evolutions of velocity (or elastic constant) in low and high pressure regions at temperatures above 450 K have been observed, similar to the transformation between LDW and HDW, in which the slope of the density dependence of the elastic constant in LDW increases with increasing temperature from 7.63 to 13.17, while that in HDW is almost invariant with temperature [16]. As the turning points in this work are located at pressure above about 2.0 GPa, much higher than that in the transition between LDW and HDW with only a few kilobars at ambient temperature, the velocity descent was observed more clearly as is shown in figure 2. From the resemblance in elastic changes in liquid water, there may be another density change in the higher temperature and pressure regime, which means the possibility of multiple liquid–liquid transitions in a stable liquid regime.

The analysis of hydrogen bonding structure under HPHT conditions by various experimental studies disputes mainly about whether there is an apparent decrease or weakening of the hydrogen bond with increasing pressure or temperature [18, 19, 28–32]. For example, investigation by XRS and XAS indicated that upon heating most molecules in liquid water are in two hydrogen-bonded configurations with one strong donor and one strong acceptor hydrogen bond, in contrast to the four hydrogen-bonded tetrahedral structure; however these findings partly contradict results from *ab initio* molecular dynamic calculations and neutron diffraction. A detailed structural interpretation pronounced the hydrogen bond remained intact; although water approaches a local structure common to a simple liquid with increasing density, it goes along an approximately constant distance above the melting line up to 6.5 GPa and 670 K. For many liquids under normal pressure, the sound velocity is a monotonically decreasing function of temperature. In the case of water, it was shown that the sound velocity first increases with temperature, goes to a maximum around 330 K, and then decreases [33–36]. When under pressure, the velocity dispersion turning point may move to higher temperature, and that is the reason we can observe an evident descent of velocity in the low pressure regime but not in the high pressure regime. In other words, we might observe the descent of velocity at pressures above 2.0 GPa if we heated it up to higher temperature. Though we are unable to get direct information on the hydrogen bonding configurations from these current measurements, we believe that the density changes reflected in these elastic measurements are induced by local structural modification to some degree.

Always regarded as an analogue of liquid water, the structure of the amorphous ices and transformations related to them have been extensively studied by various experimental and simulation methods. The discovery of the third amorphous ice, namely VHDA, in 2001 by

Loerting *et al* indicated a multiplicity of the phase transitions between amorphous ices, and indicated, although indirectly, the possibility of more than one phase transition in supercooled liquid water. As more and more computer simulations on the multiplicity of liquid–liquid phase transition in supercooled water have been presented, experimental confirmation is expected. In the stable liquid region under high pressure and high temperature multiplicity of the phase transitions was not observed in experiments or simulations. Nevertheless, we cannot exclude this possibility as we are not sure how many different local orders in liquid phases, including both metastable and stable regions, may originate from the abundant structure of the corresponding crystalline phase.

4. Conclusion

High pressure and high temperature Brillouin scattering study was performed to give an investigation of the sound velocity and elastic properties in liquid water. Two different experimental paths were adopted to measure the velocity changes with pressure and temperature respectively. From the comparison between velocity dispersion along several isothermal lines, a velocity descent with increasing temperature at pressures below about 2.0 GPa was observed, while no obvious drop was seen in the high pressure region. The results measured along the quasi-isobaric lines were consistent with that measured along isothermal lines. The velocity behavior in liquid water under HPHT conditions is related to versatile hydrogen bond configurations.

Acknowledgments

We thank Mr M Grimsditch for the data of the refractive index of water and Mr A Marco Saitta for his useful discussion of the local structure of HDW. This work was supported by the National Natural Science Foundation of China (grant Nos 10304005 and 50334030). We also acknowledge the funding assistance of the National Basic Research Program of China (grant Nos 2005CB724400 and 2001CB711201).

References

[1] Stanley H E, Buldyrev S V, Canpolat M, Mishima O, Sadr-Lahijany M R, Scala A and Starr F W 2000 The puzzling behavior of water at very low temperature *Phys. Chem. Chem. Phys.* **2** 1551–8
[2] Lobban C, Finney J L and Kuhs W F 1998 The structure of a new phase of ice *Nature* **391** 268–70
[3] Cai Y Q *et al* 2005 Ordering of hydrogen bonds in high-pressure low-temperature H_2O *Phys. Rev. Lett.* **94** 025502
[4] Finney J L, Bowron D T, Soper A K, Loerting T, Mayer E and Hallbrucker A 2002 Structure of a new dense amorphous ice *Phys. Rev. Lett.* **89** 205503
[5] Brovchenko I and Oleinikova A 2006 Four phases of amorphous water: simulations versus experiment *J. Chem. Phys.* **124** 164505
[6] Poole P H, Sciortino F, Essmann U and Stanley H E 1992 Phase behaviour of metastable water *Nature* **360** 324–8
[7] Harrington S, Zhang R, Poole P H, Sciortino F and Stanley H E 1997 Liquid–liquid phase transition: evidence from simulations *Phys. Rev. Lett.* **78** 2409–12
[8] Mishima O and Stanley H E 1998 The relationship between liquid, supercooled and glassy water *Nature* **396** 329–35
[9] Starr F W, Bellissent-Funel M C and Stanley H E 1999 Structure of supercooled and glassy water under pressure *Phys. Rev.* E **60** 1084–7
[10] Finney J L, Hallbrucker A, Kohl I, Soper A K and Bowron D T 2002 Structures of high and low density amorphous ice by neutron diffraction *Phys. Rev. Lett.* **88** 225503

[11] Loerting T, Salzmann C, Kohl I, Mayer E and Hallbrucker A 2001 A second distinct structural 'state' of high-density amorphous ice at 77 K and 1 bar *Phys. Chem. Chem. Phys.* **3** 5355–7
[12] Brovchenko I, Geiger A and Oleinikova A 2003 Multiple liquid–liquid transitions in supercooled water *J. Chem. Phys.* **118** 9473–6
[13] Loerting T, Schustereder W, Winkel K, Salzmann C G, Kohl I and Mayer E 2006 Amorphous ice: stepwise formation of very-high-density amorphous ice from low-density amorphous ice at 125 K *Phys. Rev. Lett.* **96** 025702
[14] Jedlovszky P and Vallauri R 2005 Liquid–vapor and liquid–liquid phase equilibria of the Brodholt–Sampoli–Vallauri polarizable water model *J. Chem. Phys.* **122** 081101
[15] Saitta A M and Datchi F 2003 Structure and phase diagram of high-density water: the role of interstitial molecules *Phys. Rev.* E **67** 020201
[16] Li F F, Cui Q L, He Z, Cui T, Zhang J, Zhou Q and Zou G T 2005 High pressure–temperature Brillouin study of liquid water: evidence of the structural transition from low-density water to high-density water *J. Chem. Phys.* **123** 174511
[17] Kawamoto T, Ochiai S and Kagi H 2004 Changes in the structure of water deduced from the pressure dependence of the Raman OH frequency *J. Chem. Phys.* **120** 5867–70
[18] Wernet Ph *et al* 2004 The structure of the first coordination shell in liquid water *Science* **304** 995–9
[19] Strässle Th, Saitta A M, Le Godec Y, Hamel G, Koltz S, Loveday J S and Nelmes R J 2006 Structure of dense liquid water by neutron scattering to 6.5 GPa and 670 K *Phys. Rev. Lett.* **96** 067801
[20] Mao H K, Bell P M, Shaner J W and Steinberg D J 1978 Specific volume measurements of Cu, Mo, Pd, and Ag and calibration of the ruby R_1 fluorescence pressure gauge from 0.06 to 1 Mbar *J. Appl. Phys.* **49** 3276–83
[21] Polian A 2003 Brillouin scattering at high pressure: an overview *J. Raman Spectrosc.* **34** 633–7
[22] Frank M R, Fei Y and Hu J 2004 Constraining the equation of state of fluid H_2O to 80 GPa using the melting curve, bulk modulus, and thermal expansivity of ice VII *Geochim. Cosmochim. Acta* **68** 2781–90
[23] Datchi F, Loubeyre P and LeToullec R 2000 Extended and accurate determination of the melting curves of argon, helium, ice (H_2O), and hydrogen (H_2) *Phys. Rev.* B **61** 6535–46
[24] Ragan D D, Gustavsen R and Schiferl D 1992 Calibration of the ruby R_1 and R_2 fluorescence shifts as a function of temperature from 0 to 600 K *J. Appl. Phys.* **72** 5539–44
[25] Schiebener P, Straub J, Levelt Sengers J M H and Gallagher J S 1990 Refractive index of water and steam as a function of wavelength, temperature and density *J. Phys. Chem. Ref. Data* **19** 677–717
[26] Vedam K and Limsuwan P 1978 Piezo- and elasto-optic properties of liquids under high pressure. I. refractive index versus pressure and strain *J. Chem. Phys.* **69** 4762–71
[27] Saul A and Wagner W 1989 A fundamental equation for water covering the range from the melting line to 1273 K at pressures up to 25 000 MPa *J. Phys. Chem. Ref. Data* **18** 1537–64
[28] Soper A K and Ricci M A 2000 Structures of high-density and low-density water *Phys. Rev. Lett.* **84** 2881–84
[29] Soper A K 2000 The radial distribution functions of water and ice from 220 to 673 K and at pressures up to 400 MPa *Chem. Phys.* **258** 121–37
[30] Krisch M *et al* 2002 Pressure evolution of the high-frequency sound velocity in liquid water *Phys. Rev. Lett.* **89** 125502
[31] Bellissent-Funel M-C and Bosio L 1995 A neutron scattering study of liquid D_2O under pressure and at various temperatures *J. Chem. Phys.* **102** 3727–35
[32] Schwegler E, Galli G and Gygi F 2000 Water under pressure *Phys. Rev. Lett.* **84** 2429–32
[33] Greenspan M and Tschiegg C E 1957 Speed of sound in water by a direct method *J. Res. Natl Bur. Stand.* **59** 249–54
[34] Trinh E and Apfel R E 1978 The sound velocity in metastable liquid water under atmospheric pressure *J. Chem. Phys.* **69** 4245–51
[35] Rouch J, Lai C C and Chen S H 1976 Brillouin scattering studies of normal and supercooled water *J. Chem. Phys.* **65** 4016–21
[36] Hareng M and Leblond J 1980 Brillouin scattering in superheated water *J. Chem. Phys.* **73** 622–5